Available online at www.sciencedirect.com

SCIENCE DIRECT®

Materials Letters 59 (2005) 2821 – 2826

materials letters

www.elsevier.com/locate/matlet

Preparation and characterization of dielectric glass-ceramics in $Na_2O-PbO-Nb_2O_5-SiO_2$ system

Jun Du, Beth Jones, Michael Lanagan*

Materials Research Institute, The Pennsylvania State University, University Park, PA 16802, USA

Received 7 January 2005; accepted 27 February 2005
Available online 23 May 2005

Abstract

Glass-ceramics in the $Na_2O-PbO-Nb_2O_5-SiO_2$ system have been synthesized to produce bulk materials with nanometer-sized crystals grown in a glass phase via roll-quenching followed by controlled crystallization. X-ray diffraction studies indicate that $Pb_2Nb_2O_7$, $NaNbO_3$ and $PbNb_2O_6$ phases are formed from the as-quenched glass in temperature range from 750 to 900 °C. $Pb_2Nb_2O_7$ crystallizes at 750 °C and disappears at 850 °C, $NaNbO_3$ is the primary phase at 850 °C, while $PbNb_2O_6$ is formed at a higher temperature of 900 °C. The dielectric properties of the glass-ceramics formed through controlled crystallization have a strong dependence on the phase assemblages that are developed during heat treatment. The highest dielectric constants (>600) were found in samples annealed at 850 °C for 3 h. Microstructural observation shows that randomly oriented, nanometer-sized crystalline are found with residual glass concentrated at crystallite boundaries. Further studies by scanning tunneling electron microscopy (STEM) in conjunction with energy dispersive spectroscopy (EDS) reveals inhomogeneous distribution of $NaNbO_3$ and $PbNb_2O_6$ in the sample annealed at 850 °C for 3 h and these phases contribute to the high dielectric constant.

Keywords: Dielectric properties; Microstructure; Niobate; Glass-ceramic; Dielectrics

1. Introduction

Glass-ceramics are composites that are created through controlled crystallization of an appropriate glass composition [1]. Owing to the excellent adjustability of compositions and microstructures, glass-ceramics containing crystallines of high permittivity dispersed within glass phase make these materials strong candidates for the applications in high energy capacitors over the crystalline ferroelectrics [2].

The methods often used to synthesize dielectric materials for high energy density application are (i) sintering of dielectric ceramics powder and (ii) controlled crystallization [3]. Significant progress has been made by sintering of dielectric powders. However, the pores created during organic binder burnout and sintering are major sources of structural defects, and may result in severe property degradation and ultimately failure of the devices, which affects the capability for storing high density of energy [4]. In contrast with the conventional sintering technique, controlled crystallization offers a tractable process to synthesize pore-free glass-ceramics [5], which begins with melt-casting a glass and then heat-treating of the as-quenched glass. High dielectric constant crystalline phases are precipitated from the glass matrix during isothermal treatments. Crystallite size and the phase content can be controlled through changing relative content of glass former and metal oxides that promote nucleation and crystallization. Consequently, the dielectric constant and the breakdown strength of glass-ceramic materials are potentially very high, which will result in significant improvement in energy density.

Studies on glass-ceramics for capacitor application through controlled crystallization have been carried out by a number of authors. Most have focused on the synthesis of glass-ceramics with single crystal phase, such as $PbTiO_3$

* Corresponding author. Tel.: +1 814 8656992; fax: +1 814 8652326.
E-mail address: mxl46@psu.edu (M. Lanagan).

0167-577X/$ - see front matter © 2005 Elsevier B.V. All rights reserved.
doi:10.1016/j.matlet.2005.02.090

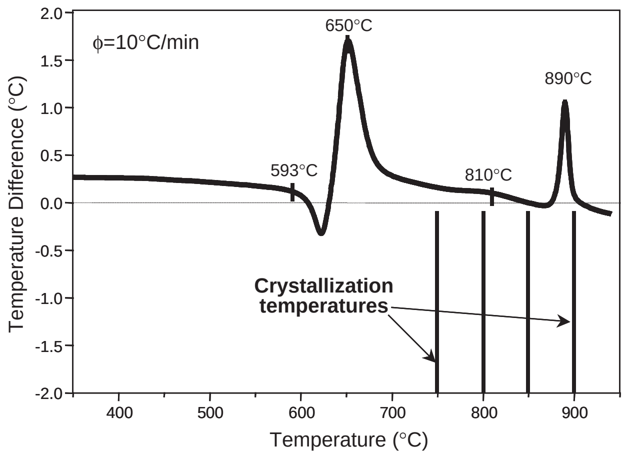

Fig. 1. DTA profile of as-quenched $Na_2O-PbO-Nb_2O_5-SiO_2$ glass.

[6], $BaTiO_3$ [7,8] and $NaNbO_3$ [9] crystallized from glass. Preparation of glass-ceramics with two ceramic phases in the system of $Na_2O-PbO-Nb_2O_5-SiO_2$ is the focus of the present paper. Particular attention has been paid to the glass-ceramics containing $NaNbO_3$ and PbNb2O_6 phases based on the studies of dielectric property of $NaNbO_3-PbNb_2O_6$ solid solution performed by Reznichenko et al. [10,11]. The correlation between the dielectric performance and microstructure of the polyphase glass-ceramics is discussed.

2. Experimental procedures

The compositional selection for forming $Na_2O-PbO-Nb_2O_5-SiO_2$ glass-ceramics was based on the pioneering work [12]. The nominal composition of the present work is 22.6 Na_2O–11.3 PbO–45.1 Nb_2O_5–21 SiO_2 in cation mole percentage. Well-mixed oxide powders containing appropriate amounts of the above compositions were melted in a platinum crucible for 2–3 h at ~1500 °C. The initial glasses were formed by rapid melt-quenching. In this work, a melt-rolling process was used, which consists of passing the melt between two cold stainless steel rolls to form 0.3~0.5 mm thick glass sheets. The glass sheets then were immediately placed in an annealing oven at 650 °C and held for 2 h to reduce internal stress before furnace-cooling to room temperature. The controlled crystallization of glass was carried out in air over temperature range from 750 to 900 °C for 10–180 min.

Approximately 0.5 g of ground glass was used for differential thermal analysis (Model SDT 2960, TA Instruments, New Castle, DE), which was heated to 900 °C at the rate of 10 °C/min. Based on the crystallization temperature determined by DTA, a series of isothermal treatments were carried out in the temperature range of 750~900 °C, and the developed phases were identified from powder X-ray diffractometry (XRD) patterns (Model Pad V, Scintag Inc., Cupertino, CA). Scans were recorded at room temperature over a 2θ range of 20~90° at a scan rate of 0.02/2 s.

The measurements of dielectric constant and dielectric loss for glass-ceramics were performed using 4284A precision LCR meter (Agilent) in the temperature range of −25~150 °C and frequency range of 100 Hz~1 MHz. Gold electrodes were sputter-deposited on both sides of the glass-ceramic sheets.

Transmission electron microscopy (TEM) is used in a complementary fashion to XRD to provide more detailed microstructural and microchemistry information of glass-ceramics in $Na_2O-PbO-Nb_2O_5-SiO_2$ system. TEM sam-

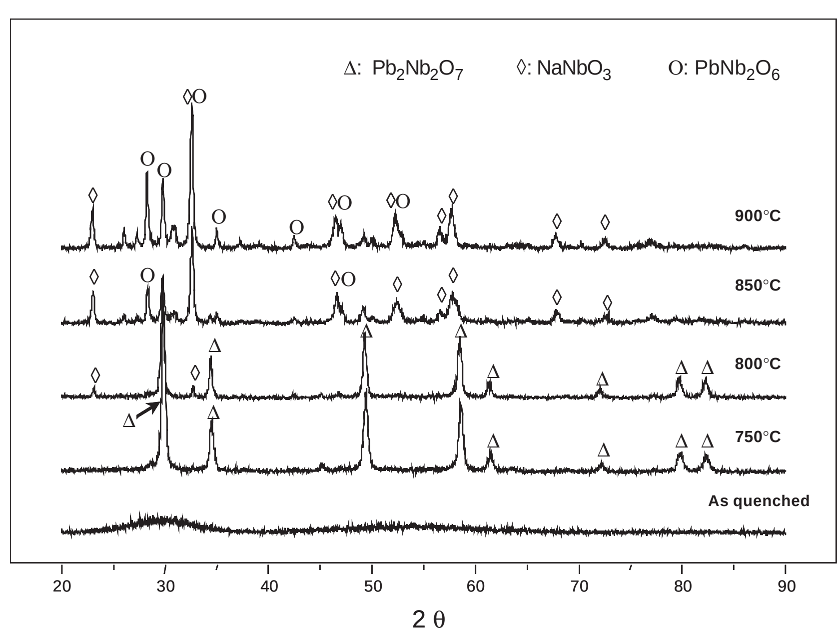

Fig. 2. XRD patterns of the as-quenched glass and glass-ceramics in $Na_2O-PbO-Nb_2O_5-SiO_2$ system.

ples were prepared following traditional procedures including mechanical polishing and ion milling. Ion milling was performed using an EAF Model 3000 Ion Mill operating at 4∼5 kV and 5 mA with an inclination angle of 10∼12°. The samples were cooled to a liquid-nitrogen temperature during ion milling to minimize possible structural transformation from glass matrix. The studies of microstructure and microchemistry of the glass-ceramics were performed using a JEOL transmission electron microscope equipped with a field emission gun (JEOL 2010F) operating at 200 kV. Energy dispersive spectroscopy (EDS) was carried out with the Emispec system in scanning transmission electron microscopy (STEM) mode. The electron probe diameter is ∼1 nm.

3. Results and discussions

3.1. Crystallization

Heat treatment protocols for the as-quenched glass were guided by DTA analysis (Fig. 1). As temperature is increased to 593 °C, an endothermic dip is observed in the DTA curve, which is attributed to the softening of the glass. Upon further increase of temperature, three exothermic peaks are observed with maximum intensities located at 650, 810 and 890 °C, respectively. The appearance of these exothermic peaks is associated with the crystallization of different phases from glass matrix [13]. Therefore, four temperatures, as indicated in Fig. 1, are chosen to investigate the crystallization behavior of the glass-ceramic material.

Phase evolution during crystallization of glass was tracked by XRD analysis. Fig. 2 shows the XRD analysis of the samples crystallized at different temperatures for 3 h. A typical amorphous feature of the as-quenched glass sample, a broad peak at about 30° (2θ), is shown in Fig. 2a. When glass is heat-treated at 750 °C, a new phase, $Pb_2Nb_2O_7$, with perovskite slab structure appears in the glass matrix (Fig. 2b). All peaks are indexed as $Pb_2Nb_2O_7$ structure, which is consistent with the DTA peak at 650 °C shown in Fig. 1. In addition, a slight peak shift toward a higher angle is observed, which could be associated with a slight decrease in lattice parameter due to substitution of Pb by Na (see Fig. 7). For the sample annealed at 800 °C, $Pb_2Nb_2O_7$ is still the primary crystal phase, while a small amount of $NaNbO_3$ begins to crystallize (Fig. 2c). The formation of $NaNbO_3$ phase is consistent with the second exothermal peak in the DTA curve that appears at 780 °C and with the maximum intensity around 810 °C. When the temperature is further increased to 850 °C (Fig. 2d), $Pb_2Nb_2O_7$ phase completely disappears. The major crystal is $NaNbO_3$ in the glass-ceramic annealed at 850 °C although the peaks are indexed as $NaNbO_3$ and $PbNb_2O_6$. The third phase, $PbNb_2O_6$, has orthorhombic tungsten bronze structure. The high temperature phases, $NaNbO_3$ and $PbNb_2O_6$, co-exist in the samples thermally treated at 900 °C (Fig. 2e). The amount of $PbNb_2O_6$ crystal in the sample annealed at 900 °C is higher than that treated at 850 °C, as shown by the relative peak intensities associated with $NaNbO_3$ and $PbNb_2O_6$ phases. The summary of crystallization sequence from glass matrix and phase constitutes in final glass-ceramics samples annealed at different temperatures is given in Table 1.

Table 1
Crystallized phases in Na_2O–PbO–Nb_2O_5–SiO_2 glass-ceramic annealed at different temperatures for 3 h

Annealing temperature (°C)	Crystallization status
As-quenched	amorphous
750	$Pb_2Nb_2O_7$
800	$Pb_2Nb_2O_7$+$NaNbO_3$
850	$NaNbO_3$+$PbNb_2O_6$
900	$NaNbO_3$+$PbNb_2O_6$

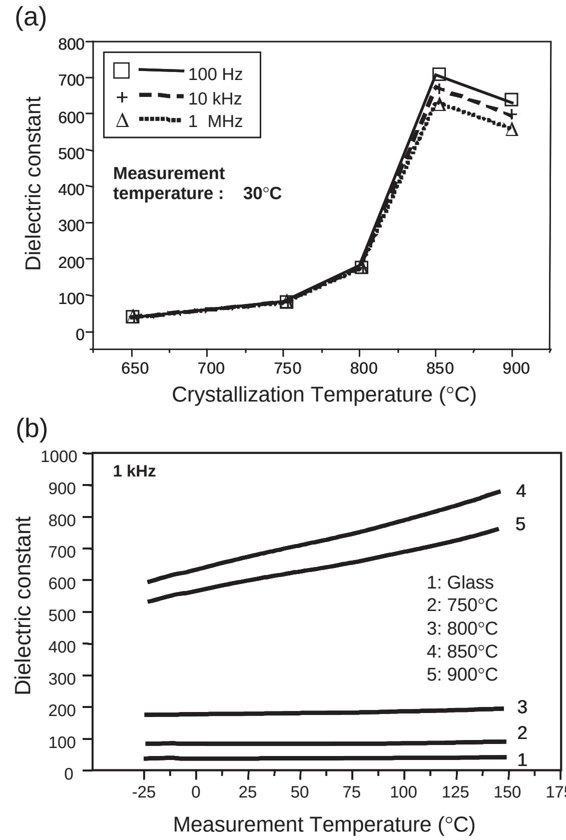

Fig. 3. (a) Dielectric constants as function of crystallization temperatures. (b) Temperature dependence of dielectric constant for samples treated at different crystallization temperatures for 3 h.

3.2. Dielectric behavior

Fig. 3(a) shows the variation of the dielectric constant as function of crystallization temperature. The dielectric constant of the as-quenched glass is about 40. Compared with other glass systems, the value of the dielectric constant is relatively high [14]. This may be attributed to that the as-quenched glass contains about 79 mol% of highly polarizable ions. Upon further heat treatment,

Table 2
Niobate dielectric ceramics and their dielectric constants

Dielectric ceramic	Dielectric constant(1 kHz, 300 K)	Reference
$PbNb_2O_6$	130∼150	[15]
$NaNbO_3$	∼500–600	[16]
$Pb_2Nb_2O_7$	∼140	[17]

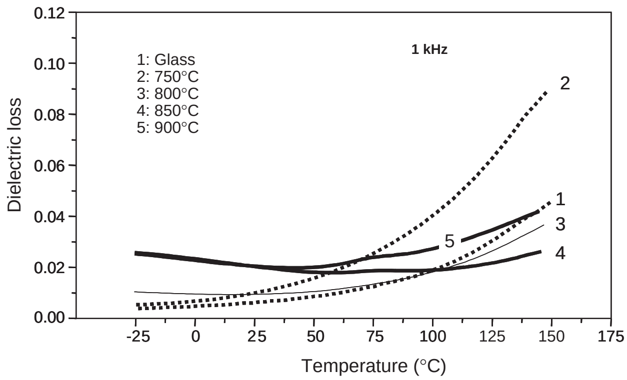

Fig. 4. Temperature dependence of dielectric loss for samples treated at different crystallization temperatures for 3 h.

the dielectric constant is increased as a result of the formation of crystal phase with high permittivity within the glass. The dielectric constant is continuously improved with the increase in crystallization temperature from 750 to 850 °C. Particularly, a significant increase in dielectric constant is found from 800 to 850 °C. This is mainly due to the high crystallization rate of high-ε_r $NaNbO_3$ at this temperature range. However, a decrease in dielectric constant is observed when the temperature is further increased to 900 °C, which may be related to the increase in the amount of $PbNb_2O_6$ phase. The dielectric property results are clearly related to the type and content of crystal phases contained in the glass-ceramic samples. The dielectric properties of the ceramic phases have been previously determined in the ($Pb_2Nb_2O_7$, $NaNbO_3$ and $PbNb_2O_6$) and are listed in Table 2. The highest dielectric constant of the sample treated at 850 °C is due to the presence of an optimum amount of $NaNbO_3$ and $PbNb_2O_6$ phases and/or their solid solutions.

Shown in Fig. 3b is the temperature dependence of dielectric constant (ε_r) at 1 kHz for samples after crystallization treatment. Temperature independent dielectric properties were observed for the samples treated at temperature below 800 °C as well as the as-quenched glass. A strong temperature dependence of the dielectric constant is clearly seen for samples heat-treated at 850 and 900 °C. The enhancement of about 50% in dielectric constant is observed when the temperature of measurement changes from −25 to 150 °C. The strong temperature dependence of dielectric constant for the glass-ceramics annealed at 850 and 900 °C is possibly associated with the phase transition from one orthorhombic (Pbma) to another orthorhombic (Pmnm) of $NaNbO_3$ phase around 365 °C [18].

Furthermore, the dielectric constant measured at 1 kHz for the glass-ceramic treated at 850 °C for 3 h is about 600∼700. This value is compatible with the previously published results obtained from sodium niobate ceramics [16]. In current glass-ceramic sample, there are 21 mol% of glass former SiO_2 and certain amount of $PbNb_2O_6$ crystal in addition to $NaNbO_3$ phase. Both SiO_2 glass former and $PbNb_2O_6$ crystal are components of lower dielectric constant. Thus, the high dielectric permittivity of the glass-ceramic annealed at 850 °C would be owing to the formation of $NaNbO_3$–$PbNb_2O_6$ solid solution [10,11].

Fig. 4 shows the temperature dependence of the dielectric loss of different glass-ceramics at frequency of 1 kHz in the temperature range of −25∼150 °C. In general, the samples crystallized at 850 and 900 °C show better stability over the temperature range of measurements. The sample treated at 850 °C, that has the highest dielectric constant, shows the lowest dielectric loss value around 50 °C.

3.3. Microstructure and microchemistry analysis

The microstructure and microchemistry in pure glass and final glass-ceramic states were studied by analytical transmission electron microscopy (TEM). Fig. 5(a) is a bright-field TEM micrograph of as-quenched glass. The insert in Fig. 5(a) corresponds to the selected area electron diffraction (SAED) pattern. The pattern is a diffuse halo, indicating a fully amorphous state of the as-quenched sample. The glassy nature of the as-quenched sample is also demonstrated in the high-resolution TEM image shown in Fig. 5(b). In fact, contrast fluctuation associated with phase separation in as-quenched glass is clearly seen in Fig. 5(a). The phase separation at the melting temperature suggests immiscibility during the melt-quench process. The phase separated regions in as-quenched glass sample are on a scale of about 5∼10 nm (Fig. 5(a)). It is expected from the bright-field image that the darker areas are rich in Pb since it is the heaviest scatterer in this system, brighter areas rich in element with lowest atomic number

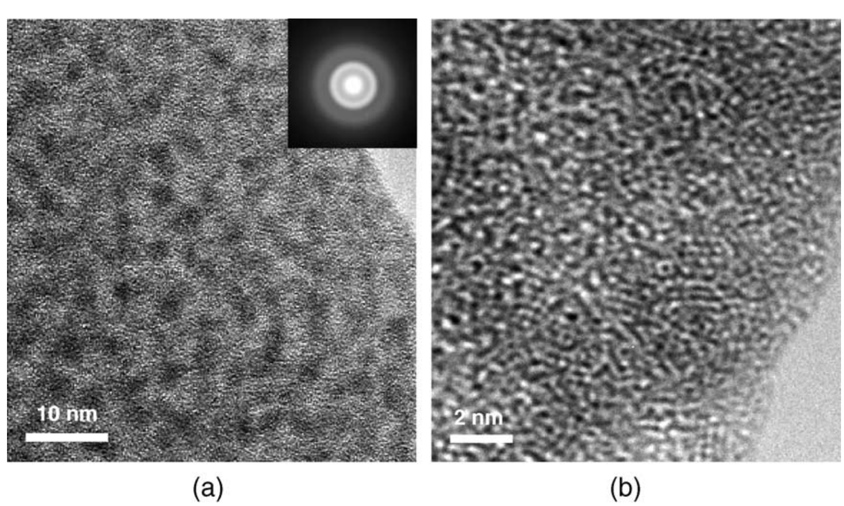

Fig. 5. Bright-field TEM micrograph (a) and HRTEM image (b) of the as-quenched glass.

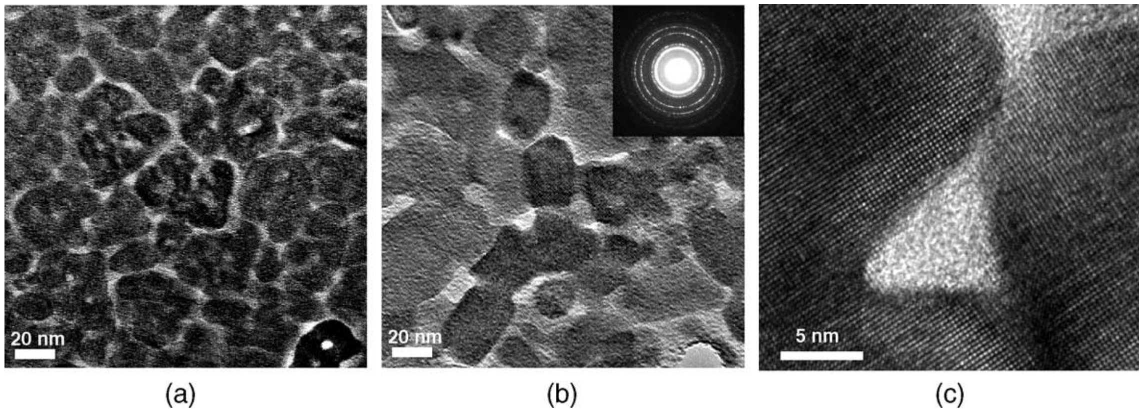

Fig. 6. (a)–(b) Bright-field TEM micrographs of the glass-ceramics treated at 850 °C for 10 and 180 min. (c) HRTEM image obtained from the glass-ceramic heat-treated at 850 °C for 180 min, showing the primary location of the residual glass.

Z of cation (Na). Such phase separated regions may serve as the nucleation sites during the crystallization process of glass and will account for the phase development sequence during annealing [19].

In Fig. 6(a)–(b) are bright-field TEM micrographs of the samples after heat treatments at 850 °C for 10 and 180 min. Darker and brighter regions correspond to crystal phases and residual glass, respectively. Different stages of crystallization are evident in the micrographs. In an early stage of crystallization of glass (Fig. 6a), the randomly oriented and nanometer-sized crystallites are surrounded by residual glass phase. The crystal grains are uniformly dispersed, suggesting that the rate of nucleation is relatively high, and the transformation of glass phase to crystalline phase is therefore completed with a minimum of time. With longer annealing, the particles tend to grow and coalesce to about 10–40 nm in size and the grain boundaries are reconstructed to regular shape, as is evident in the micrograph (Fig. 6b), while the volumetric fraction of the crystallized ceramic particles is not significantly improved. The selected area diffraction pattern inserted in the image in Fig. 6b is in form of thin diffraction rings, indicating the polycrystalline nature of the particles. All of the diffraction rings could be indexed as polycrystalline $NaNbO_3$ and $PbNb_2O_6$ phases. Fig. 6c is a HRTEM image obtained from the glass-ceramic sample annealed at 850 °C for 180 min. The residual glass is located between adjacent ceramic particles and at triple junctions, which is important for high dielectric constant.

Microchemistry of glass-ceramic samples was analyzed using STEM as complementary studies of the microstructure. A typical dark field STEM image of the sample annealed at 850 °C for 3 h is shown in Fig. 7a. The brightness of image varies from one area to another. The regions can be grouped as bright, gray and dark ones. The dark network is correlated to the residual glass in the glass-ceramic composite. The bright or gray particles form a cluster-like structure consisting of up to ~10 particles. EDS analysis was performed to elucidate the microchemical nature of the crystallized particles and the glass network in the sample.

Fig. 7b shows the EDS profiles obtained from dark (i), gray (ii) and bright (iii) areas. The distinct peaks are designated for the primary elements. As expected, oxygen peak appears in spectra (i) through (iii). The dark glass-network consists mainly of Si and O, with a small trace of Nb. This result suggests that the crystallization process is close to completion and that the glass

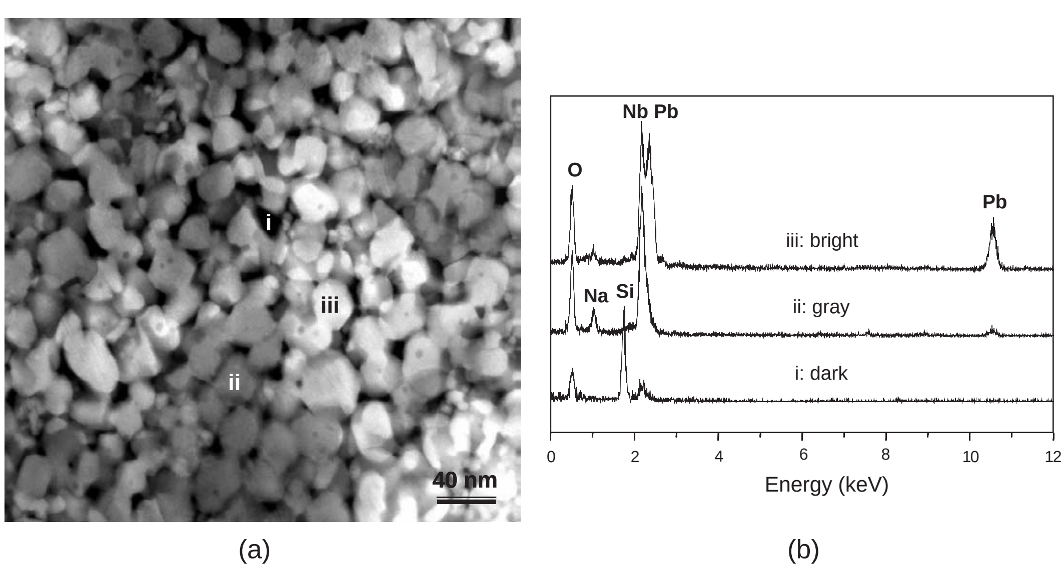

Fig. 7. (a) Dark field STEM image of the sample annealed at 850 °C for 180 min, showing local clustering of identical crystallines. (b) EDS profiles obtained from bright, gray and dark areas in Fig. 7a.

phase is distributed as isolated pockets in the polyphase assemblage. In the spectrum obtained from the bright areas, Pb and Nb are present as dominant elements. Combined with the XRD results, it is concluded that the bright areas correspond to $PbNb_2O_6$ phase. The gray regions are $NaNbO_3$ crystal phase as Na and Nb are the dominant elements in spectrum (ii). Also, it is noted from the EDS profile (ii) of the gray particle that a certain amount of Pb element exists in $NaNbO_3$ crystal phase, suggesting the formation of $NaNbO_3-PbNb_2O_6$ solid solution. The microstructure clearly shows strong connectivity of high dielectric constant crystallites, which corresponds to the high overall dielectric constant of the polyphase assemblage. Future research will focus on the dielectric properties of the solid solution and on the effects of crystal size on the dielectric properties.

4. Conclusions

Glass-ceramics for dielectric application is studied in the $Na_2O-PbO-Nb_2O_5-SiO_2$ system. In the as-quenched glass, there exists a fluctuation in local chemistry associated with glass phase separation. Three crystalline phases, $Pb_2Nb_2O_7$, $NaNbO_3$ and $PbNb_2O_6$, are formed during thermal treatment in the temperature range from 750 to 900 °C. In addition to the enhancement for dielectric constant through crystallization, it is found that dielectric constant of glass-ceramics can be tailored through controlling the nature of the crystallized phases. The glass-ceramics annealed at 850 °C for 3 h displays the best dielectric performance, which is attributed to the presence of $NaNbO_3$ and/or $NaNbO_3-PbNb_2O_6$ solid solution. The crystals of $NaNbO_3$ and $PbNb_2O_6$ are surrounded by residual glass phase. The distribution of $NaNbO_3$ and $PbNb_2O_6$ is in-homogeneous and micro-structural analysis indicated locally clustered regions. Volume fraction of the crystal phase, grain size and the connectivity are critical parameters dictating the properties of the glass-ceramics.

Acknowledgments

This work was supported by the Freedom Car Program of the U. S. Department of Energy and the Office of Naval Research.

References

[1] G.H. Beall, J. Mater. Educ. 14 (1992) 315.
[2] A. Herczog, IEEE Trans. Parts Hybrids Packag. PHP-9 (1973) 247.
[3] A.J. Moulson, J.M. Herbert, Electroceramics—Materials, Properties and Applications, Wiley, England, 2003.
[4] R. Gerson, T.C. Marshall, J. Appl. Phys. 30 (1959) 1650.
[5] M.M. Layton, A. Herczog, Glass Technol. 10 (1969) 50.
[6] T. Kokubo, M. Tashiro, J. Non-Cryst. Solids 13 (1973/74) 328.
[7] D. McCauley, R.E. Newnham, C.A. Randall, J. Am. Ceram. Soc. 81 (1998) 979.
[8] A. Bhargava, J.E. Shelby, R.L. Snyder, J. Non-Cryst. Solids 102 (1988) 136.
[9] A. Herczog, J. Am. Ceram. Soc. 73 (1990) 2743.
[10] L.A. Reznichenko, N.V. Dergunova, O.N. Razumovskaya, L.A. Shikina, Inorg. Mater. 37 (2001) 1302.
[11] L.A. Reznichenko, L.A. Shilkina, O.N. Razumovskaya, S.I. Dudkina, E.S. Gagarina, A.V. Borodin, Inorg. Mater. 39 (2003) 139.
[12] U.S. Patent number 905 253 (1962).
[13] P.W. McMillan, Glass-ceramics, Academic Press, London, 1964.
[14] P.J. Harrop, J. Mater. Sci. 4 (1969) 370.
[15] A.V. Turik, G.I. Khasabova, L.K. Chernysheva, M.L. Sholokhovich, V.E. Dugin, Sov. Phys., Solid State 26 (1984) 1406.
[16] M. Pisarski, Acta Phys. Pol., A 57 (1980) 693.
[17] J.K. Hulm, Phys. Rev. 92 (1953) 504.
[18] L.E. Cross, B.T. Nicholson, Philos. Mag. 46 (1955) 453.
[19] A. Herczog, Glass Technol. 10 (1969) 50.